EPJ Web of Conferences **137**, 09008 (2017) DOI: 10.1051/epjconf/201713709008
XIIth Quark Confinement & the Hadron Spectrum

Hades experiment probing baryonic matter at SIS18 overview of results

Piotr Salabura for the HADES collaboration[1,a]

[1] *Jagiellonian University*

Abstract. HADES experiment at GSI is the only high precision experiment probing nuclear matter in the beam energy range of a few AGeV. Pion, proton and ion beams are used to study rare dielectron and strangeness probes to diagnose properties of strongly interacting matter in this energy regime. Selected results from $p + A$ and $A + A$ collisions are presented and discussed.

1 Introduction

In the recent years a significant grow of the interest in nuclear collisions at lower energies is observed. Dedicated experimental programs of Beam Energy Scan at RHIC and NA61-SHINE at CERN are under way to search for the onset of deconfinement and for a critical point in the phase diagram of nuclear matter. New experimental facilities FAIR at Darmstadt [1] and NICA in Dubna [2] are under construction to scan the lower energy regime. This enormous activity is motivated by the very challenging but fundamental question of the understanding of structure and phases of strongly interacting matter. At high temperature and zero $\mu_b$lattice QCD, has provided strong evidence that the transition from a hadron gas to a partonic phase is a smooth crossover for physical quark masses. One expects that this crossover continues at non-zero μ_b and eventually ends in the critical point. Furthermore, it has been shown that at vanishing μ_b the phase transition is associated by another fundamental phenomenon, the restoration of chiral symmetry which is spontaneously broken in vacuum. It has also been suggested that beyond the critical point the restoration of chiral symmetry could fall apart from the transition to deconfined matter, giving rise to a confined phase with partially restored chiral symmetry. This "Quarkyonic" matter appears in the QCD limit of a large number of flavours and can be understood as a gas of confined quarks with a rich excitation spectrum. At very high μ_b and low temperatures condensation of quark pairs can take place and lead to formation of colour super-conductive phase. This gives rise to a rich phase structure in that region, depending on the various flavour-colour symmetry structures, the so-called Colour-Flavour-Locking scenarios (for more details see [3], [4]). Such phase may also exist inside the neutron stars and hence are of interest also for astrophysics. Although, in this range of T,$\mu_b$lattice QCD calculations are so far impossible, approaches based on QCD-inspired effective models are in use and provides some guidance. In this context experimental input is of largest importance to provide some constraints and to drive developments in this field.

[a] piotr.salabura@uj.edu.pl

HADES at SIS18 at GSI Darmsatdt is currently the only experiment studying properties of strongly interacting matter in a few AGeV energy regime. The strategy of the experiment is to use rare and penetrating probes like dielectrons and hadrons containing strangeness to diagnose the phase diagram at high μ_b and moderate temperatures. Using the variety of proton, deuteron, secondary pion and ion beams HADES experiments are ideally suited for systematic studies. Using heavy ion reactions a dense (up to $3\rho_0$) and hot (with temperatures up to T=80 MeV) fireball with relatively long life time ($\sim$ 10 fm/c) can be created. Experiments with pion and proton beams also allow for the study of cold-matter effects. Further experiments at SIS100 at FAIR also planned and will cover, together with the new CBM detector the $8-10$ AGeV energy range and bridge to the energy domain of BES at RHIC and SPS.

2 Experimental programme of HADES

The HADES programme realized so far can be divided into three reaction classes. Experiments studying dielectron, pion and baryon resonance productions in proton-proton (at 1.25, 2.2 and 3.5 GeV), $d + p$ (at 1.25 AGeV) and recently $\pi - p$ reactions provided important constraints on contributions of various e^+e^- sources and allowed to establish model independent reference spectra for studies of proton-nucleus and nucleus-nucleus collisions. Studies of $p + p$ collisions at 3.5 GeV provided also valuable new data on hyperon, $\Sigma(1385)$ and $\Lambda(1405)$ production. In particular measurements of the mass distribution of $\Lambda(1405)$ shows differences as compared to the one obtained from photon and pion induced reactions and calls for explanation particularly in the context of the on-going discussion about possible molecular nature of this resonance. Using Partial Wave Analysis excitation of baryon resonances via one pion and $pK^+\Lambda(1192)$ final states have been determined for proton-proton collisions (for recent review and references see [5]). These studies provide also an important input to transport model calculations where the pion and kaon production in nuclear matter is strongly influenced by couplings of the Δ, N^* resonances.

The dielectron, neutral kaon and hyperon productions were investigated in $p + Nb$ collisions at 3.5 GeV. Small $C + C$, medium size $Ar + KCl$ and recently $Au + Au$ collision systems were explored in the $1-2$ AGeV energy range to study emissivity of nuclear matter and strangeness production (ϕ, $K^{-,+,0}$, Λ, $\Xi^-(1321)$). Below we present highlights of the results obtained in $p + A$ and $A + A$ collision systems

3 Results from p+A collisions

$p + Nb$ collisions at a beam energy of 3.5 GeV have been studied by HADES with the main goal of searching for in-medium modification of vector mesons in cold nuclear matter [6]. The large acceptance of the detector and the low energy of the beam allow for a detection of e^+e^- pairs down to low momenta ($p_{e^+e^-} < 1.0$ GeV/c) which was not possible in the similar experiments performed by CLAS/JLAB (with photon beams [7, 8]) and E325/KEK [9] collaborations. Differential e^+e^- production cross sections as a function of the e^+e^- invariant mass (shown in Fig. 1), the momentum and the rapidity have been measured and compared to those obtained from $p + p$. The direct comparison of the measured distributions to the yields expected from the known hadronic sources (from a PYTHIA calculation) is shown for $p + p$ collisions in Fig. 1 [10]. It reveals an unexplained strength below the vector meson pole which becomes even more pronounced in the proton-nucleus collisions. Such additional strength can be explained by a strong coupling of the ρ meson to low-mass baryonic resonances,

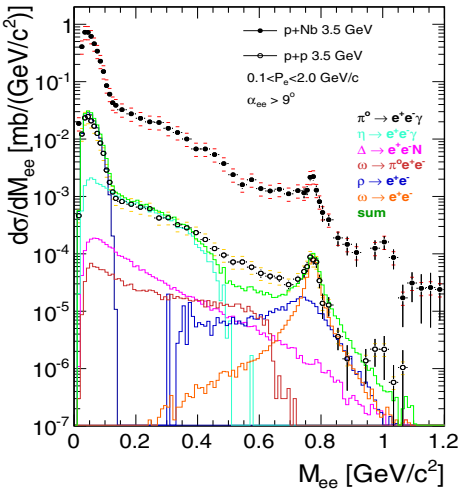

Figure 1. Comparison of dielectron cross sections as a function of the invariant mass measured in $p+p$ and $p+Nb$ collisions at beam energy of 3.5 GeV. For the $p+p$ data, a PYTHIA dilepton cocktail composed of various e^+e^- sources, defined in the legend, is displayed in addition [6, 10]

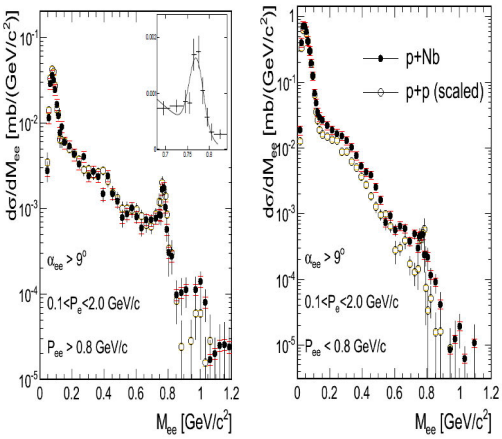

Figure 2. Comparison of the invariant mass spectra for e^+e^- pairs with $p_{e^+e^-} > 0.8$ GeV/c (left panel) from $p+p$ and $p+Nb$. The inset shows a linear zoom into the vector meson region together with a fit to the ω peak for the p+Nb data. Right: for pairs with $p_{e^+e^-}$ <0.8 GeV/c. The $p+p$ data have been scaled as described in the text [6]

which was not included in PYTHIA. Modification of the invariant mass spectrum are expected due to electromagnetic transition form factors of $R \rightarrow Ne^+e^-$ decays which according to Vector Meson Dominance (VDM) proceed via intermediate vector mesons. Indeed, calculations [11, 12] including the form factors of $\Delta \rightarrow Ne^+e^-$ obtained from the two component model [13], and contributions from higher mass resonances $N^* \rightarrow \rho N \rightarrow e^+e^-N$ describe the missing yield. However, this result has to be taken with caution since the exact production cross sections of the resonances and their decay branches into ρN are subject to large uncertainties. It is expected that the recently collected data on dielectron and pion production in $\pi - p$ reaction channels and the planned future campaigns with the pion beam (see contribution of F.Scozzi to this conference) will shed more light on this important aspect.

Coming back to the $p+Nb$ data, we show in Fig. 2 the comparison of the e^+e^- invariant mass distribution to the one measured in $p+p$ reactions for two momentum bins of the outgoing dielectron pair. Here, the $p+p$ cross sections have been scaled up by the ratio of the total cross sections for both reactions and the averaged numbers of participants calculated with a Glauber model: $\sigma_{pNb}/\sigma_{pp} \times < A^{pNb}_{part} > / < A^{pp}_{part} >$. With such scaling π^0 production measured in the $p+p$ describes (see Fig. 2) pion Dalitz yield in $p+Nb$. On the other hand, an increase of the e^+e^- yield below the vector meson pole above the $p+p$ reference is visible for low momenta $p_{e^+e^-} < 0.8$ GeV/c (see also Fig.3, left panel).

In order to better quantify this excess we subtract first, the ω peak in both data samples and further subtract the scaled $p+p$ dielectron yield from the $p+Nb$ yield. The difference, shown in Fig. 3-right panel, represents the additional e^+e^- radiation excess due to the medium. It shows an exponential decrease with an additional enhancement directly below the vector meson pole mass, i.e. between 0.6-0.7. Note that this enhancement is exactly at the position where a discrepancy is observed when comparing the $p+p$ data with the PYTHIA calculation (Fig. 1), indicating that both observations

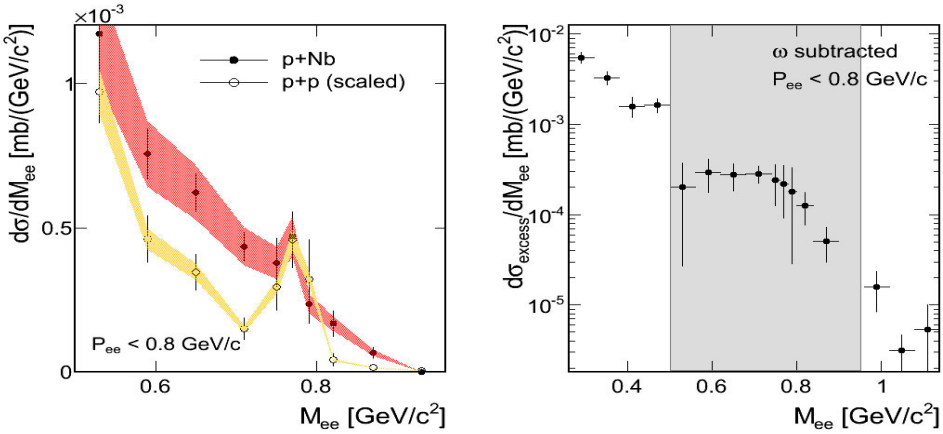

Figure 3. Left: Same as in Fig. 2 but zoomed into the vector meson region. The shaded bands represent the systematic uncertainties due to the normalization. Right: Excess yield in the $p + Nb$ data after subtraction of the scaled p+p reference data (the ω contribution has been subtracted in both data samples). The grey region corresponds to the invariant mass range plotted in the left picture

might be linked to the coupling of baryon resonances to the ρ meson. The excess observed in the case of $p + Nb$ might be interpreted as a fingerprint of the contribution of the multi-step processes processes of the type $p + p \rightarrow \pi X$, $\pi N \rightarrow R \rightarrow Ne^+e^-$ adding also to this mass region because of the aforementioned strong resonance-ρ couplings. On the other hand, model calculations based on hadronic many-body interactions also predict that such couplings strongly modify the in-medium ρ meson spectral function [14]. Therefore, final conclusions about in medium modifications of the ρ meson in cold nuclear matter can be derived only if the ρ-baryon resonance couplings are fully understood. In this context the data from pion induced reactions will play a decisive role.

As the ω meson is concerned, we observe that for slow pairs the yield at the ω pole is not reduced, however, the underlying smooth distribution is enhanced. Thus, the yield in the peak is almost zero within errors. This indicates a strong ω absorption in contrast to the pairs from the underlying continuum. Assuming that the ω cross section scales with the mass number as $\sigma_{pNb} = \sigma_{pp} \times A^{\alpha}$ we obtain α =0.38± 0.29 for slow pairs and α=0.67 ± 0.11 for $p_{e^+e^-} > 0.8$ GeV/c. Furthermore, an analysis of the ω width shows, within the error bars, no significant broadening. Both observations are in line with the results of the CBELSA-TAPS experiment [15], although one should note that in contrast to the $p + A$ reactions for the photon induced reactions no initial state effects and consequently a stronger scaling could be expected.

The large statistics collected for the $p+Nb$ system allowed also for studies of the hyperon-nucleon interactions via two-particle correlation function [16]. The $\Lambda - p$ interaction has become more and more crucial in recent years due to its connection to the modelling of astrophysical objects like neutron stars. It appears that in the inner core of the star the existence of hyperons is possible since their creation is often energetically favoured in comparison with a purely nucleonic matter composition. However, the appearance of these additional degrees of freedom leads to a softening of the nuclear

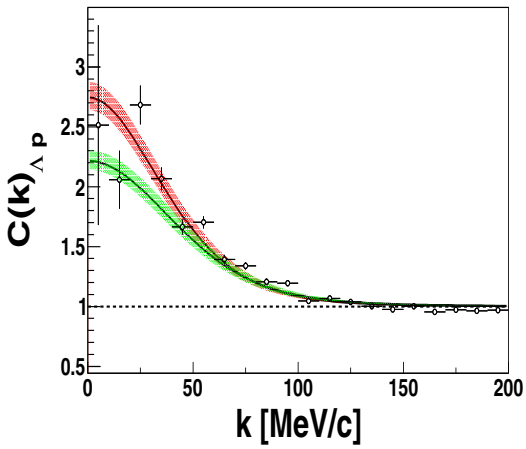

Figure 4. Comparison of the experimental $\Lambda - p$ correlation function (open circles with error bars) to the LO (green) and NLO (red) scattering parameter set (see ref [17] for details. The error bands in the theory curves correspond to the errors of the $\Lambda - p$ source size determination [16]

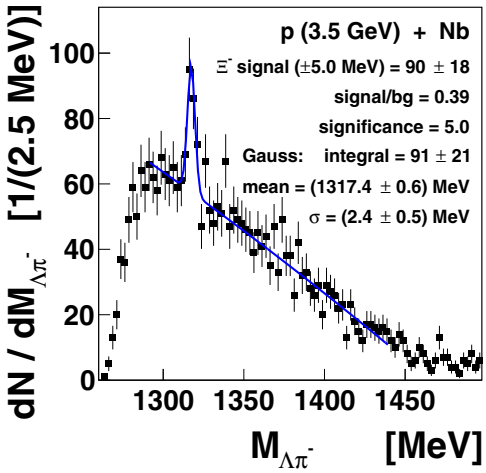

Figure 5. $\Lambda - \pi^-$ invariant-mass distribution measured in $p + Nb$ collisions at 3.5 GeV. The error bars show the statistical errors. The curve represents a combination of a Gaussian and a polynomial function used to fit the data.[18]

equation of state (EOS) incompatible with the observation of the neutron stars of two solar masses. This leads to the 'hyperon puzzle'. Many attempts were made to solve this puzzle, e.g. by introducing three-body forces leading to an additional repulsion that can counterbalance the large gravitational pressure and finally allow for larger star masses. Another possibility is offered by calculations using a chiral effective field theory approach. The results [17] with leading order (LO) and next-to-leading order (NLO) demonstrate an attractive interaction for low hyperon momenta ($p < 600$ MeV/c) but for higher momenta NLO results show a repulsive interactions. Using the femtoscopy technique we performed first studies of the scattering lengths and effective ranges for hyperon-nucleon pairs in $p+A$ collisions. The $p - \Lambda$ correlation function are shown in Fig. 4 in comparison to the calculations with LO and NLO results (both versions are plotted separately). The statistical error of data are too large to derive conclusions but shows sensitivity of the method. Future experiments are planned which thanks to the improved DAQ of HADES can provide data sample with statics larger by an order of magnitude.

Another interesting result obtained from studies of Λ particle correlations reveals a significant $\Xi^-(1321)$ peak signalling sub-threshold (70 MeV below the threshold of free $p + p$) production [18]. This observation is particularly interesting in connection with the Ξ^- signal measured in $Ar + KCl$ reactions at 1.76 GeV and will be discussed in the next section.

4 Results from A-A collisions

In the $1 - 2$ AGeV energy range, particle production in heavy-ion collisions is dominated by pion production which originates mainly from the $\Delta(1232)$ resonance. Multiplicities of heavier mesons,

mainly η, are already very low (of order 1 – 2%). Production multiplicities for π^0 and η mesons are known from their decay into real photons from former TAPS measurements at GSI [19]. The dielectron invariant-mass distributions measured with HADES in the light $C + C$ 1 and 2 AGeV collisions can be well described by a superposition of $N - N$ collisions [20]. However, radiation from the medium-heavy $Ar + KCl$ (at 1.756 AGeV) [21] systems show a significant contribution from a dense collision phase.

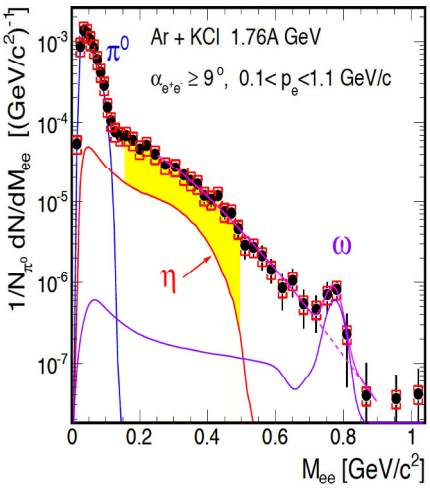

Figure 6. e^+e^- invariant mass distribution normalized to the π^0 yield measured in $Ar+KCl$ collisions at 1.76 AGeV compared to a dielectron cocktail of long lived mesonic sources (π^0, η, ω) acounting for radiation after freeze-out [21].

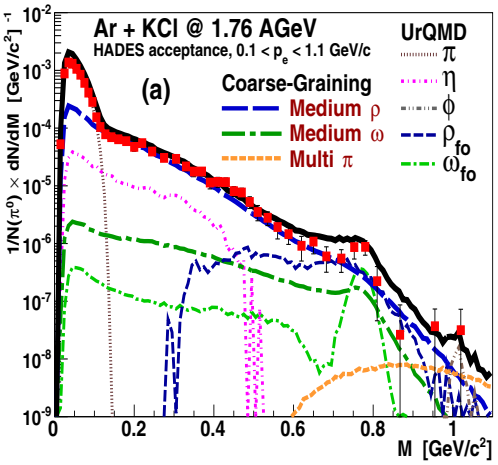

Figure 7. Similar distributions but compared to coarse-grained transport calculations which account for the radiation from dense collision phase mediated by in-medium ρ and, to smaller extent, ω meson [27].

Fig. 6 shows the dielectron invariant mass distribution normalized to the mean of the charged pion (π^+, π^-) yields, measured independently by HADES, and extrapolated to the full solid angle. At this energy and this collision system it is a good measure of neutral pion multiplicity. The differential distributions obtained in such a way are compared to the expected mesonic e^+e^- cocktail from the π^0, η Dalitz and ω decays according to the measured (for π^0 and η) and extrapolated from the m_T scaling for the ω multiplicities. One should underline that the ω peak visible in the invariant mass distribution in $Ar+KCl$ collisions constitutes the first measurement of meson production at such a low energy (below its free $N-N$ threshold). As one can see, the e^+e^- cocktail composed from the meson decays does not explain the measured yields for both collision systems and leave a room for a contribution expected from baryonic sources like Dalitz decays (mainly $\Delta(1232)$), nucleon-nucleon bremsstrahlung and in-medium radiation. The latter one appears to be a dominant source of the radiation, as shown in Fig. 7 by a coarse-grained transport calculation [27]. This contribution accounts for a thermal radiation from a fireball [28], in a similar fashion as for SPS [22, 23] and RHIC data [24, 25]. It is mainly given by a radiation from the ρ-meson with spectral function strongly modified due to the meson-baryon resonance couplings [14]. This multi-body hadronic interactions lead to a dramatic broadening of the ρ mass distribution and allows for a remarkable consistent explanation of the thermal dilepton

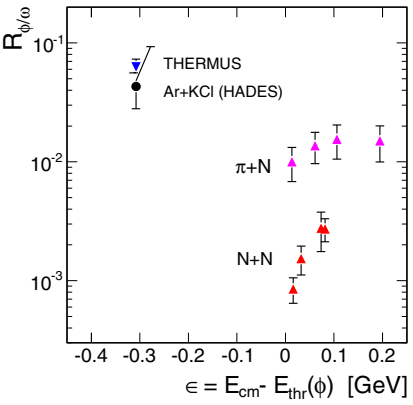

Figure 8. Comparison of the measured $R_{\phi/\omega}$ ratio (HADES) and statistical model value (THERMUS fit) as well as a compilation of data from the $p + p$ and $\pi + N$ reactions (see text). The ratio is plotted as a function of the excess energy above the threshold for the exclusive production in $p + p$ and $\pi + N$ reactions [30].

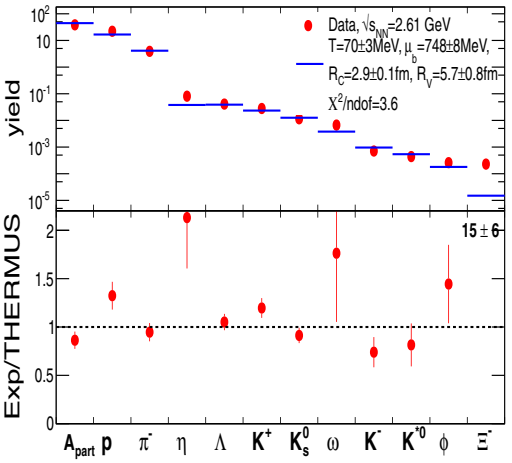

Figure 9. Yields (filled red circles) of hadrons in Ar+KCl reactions and the corresponding THERMUS fit values (blue bars). The lower plot shows the ratio of the experimental value and the THERMUS value. For the Ξ^- the ratio number is quoted instead of a point.[31].

rates over a broad energy range from SIS18 (HADES), SPS(NA60/CERES) to RHIC energies [28]. The underlying connection of the hadronic model to the chiral symmetry is nicely provided by the QCD and Weinberg sum rules relating the spectral functions of the vector (ρ) and the axial-vector (a_1) mesons, which mass splitting in vacuum is a direct consequence of the chiral symmetry breaking, with the expectation value of quark condensate also appearing due the symmetry breaking. The latter one can be calculated by lattice QCD in the limit of vanishing μ_b while the meson spectral function can be provided by the aforementioned many body hadronic theory. Using such connections, the evolution of spectral functions of the a_1 and ρ meson was calculated and shown to be consistent with chiral symmetry restoration [26].

These remarkable results nicely demonstrate penetrating nature of the dileptons which allows to observe an effect of "shining" of the baryonic matter integrated over the whole collision time. As shown by the model calculations [27, 29] the yield of radiation is a direct measure of collision time and hence can serve as a chronometer of the reaction. A further important test of this scenario will be provided by data recently obtained from $Au + Au$ collisions at 1.25 GeV where even larger yield of thermal radiation is expected.

Interesting results on the vector meson production in heavy-ion collisions at SIS18 have also been obtained from analysis of $Ar + KCl$ data. Besides the ω signal discussed above, a surprisingly strong ϕ meson production has been found from an analysis of the K^+K^- final state [30]. The acceptance corrected ϕ/K^- ratio is found to be 0.37 ± 0.13 which translates into a fraction of $18 \pm 7\%$ of negative kaons coming from ϕ decay. Furthermore, assuming that non-resonant K^+K^- production is of the same size, as it is known from $N + N$ reactions, even larger contribution of these type of reactions to the anti-kaon production can be deduced. This conclusion is further supported by the observation of the different slopes of transverse mass distributions of kaon and anti-kaon spectra which can naturally be explained as the effect of the ϕ feed-down [31]. This is surprising since strangeness exchange

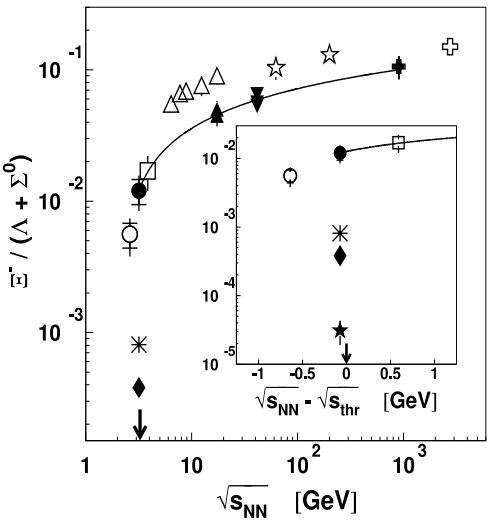

Figure 10. The excitation function of the $\Xi^-(1321)$ to $\Lambda + \Sigma^0$ ratio measured by HADES (full circles) and other high energy experiments (empty symbols) compared to statistical model predictions [37] (solid curves). The arrow depicts the $\Xi^-(1321)$ threshold [37]

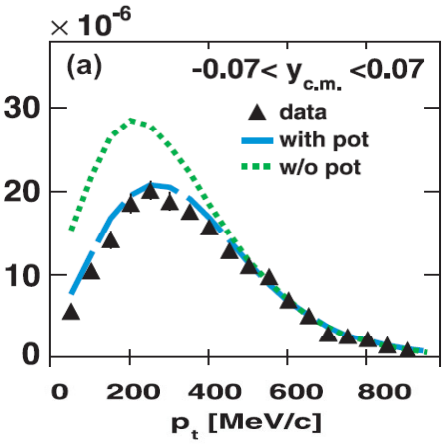

Figure 11. p_t distribution of the experimental K^0_S data (full triangles) together with the results of the IQMD model including a repulsive K^0 -nucleus potential of 46 MeV (dashed curves) and without potential (dotted curves) [42].

(π^- hyperon $\rightarrow K^-N$) has been assumed before to be the dominant process in K^- production. The HADES result indicate that the ϕ meson is also produced in multi-step processes involving short-lived resonances. Such scenario is corroborated by BUU and UrQMD transport calculations [32], [34] which reproduce the yields and spectral distributions of K^+K^- and ϕ mesons.

Fig. 8 shows the ratio of the ϕ to ω multiplicities measured in $Ar + KCl$ collisions at 1.756 AGeV, together with predictions of the statistical model THERMUS [35] and results from elementary reactions [30, 31]. The data points are plotted as a function of the excess energy above the production threshold for the exclusive ϕ production in $p + p$ and $\pi + N$ reactions, respectively. One can see from this comparison that in the heavy-ion reaction $R_{\phi/\omega}$ is more than one order of magnitude larger than in $N + N$ collisions and also at least a factor $3 - 5$ larger than in pion-induced processes. On the other hand, the ratio is consistent with the calculation of statistical thermalization model assuming no suppression due to OZI rules [31].

The ability of HADES for the selection of displaced secondary vertices arising from weak decays and the high statistics accumulated for the collision system $Ar + KCl$ at 1.76AGeV allowed to investigate the deep-subthreshold production ($\sqrt{s_{NN}} - \sqrt{s_{thr}}$ =-640MeV) of the double-strange $\Xi^-(1321)$ hyperon [37]. The $\Xi^-(1321)$ was reconstructed in the $\Lambda - \pi^-$ invariant mass distribution thanks to a high-purity signal of Λ identified in the $p - \pi^-$ invariant mass distribution. The obtained yield of the cascade has been fitted together with the other hadron yields measured by HADES by the THERMUS and the results are shown in Fig. 9. The fit describes all particle yields, except $\Xi^-(1321)$, where an enhancement of 15 ± 6 is observed. The freeze-out condition corresponds to T=70±3 MeV and the chemical potential $\mu_b = 748 \pm 8$ MeV [31] and line up with a general freeze-out line obtained from the fit to word data.

Increase of strangeness production (particularly with multi strange content) has been recently predicted to be an ideal probe for quark deconfinement in baryon-rich matter in the FAIR/NICA energy range [38]. Hence pioneering results on Ξ^- production of HADES are of large importance. In the works [39],[40] the strong $\Xi^-(1321)$ production observed in $Ar + KCl$ collision system has been accounted for by strangeness exchange reactions of the type hyperon-hyperon $\rightarrow$ N$\Xi^-(1321)$, where hyperons are produced in the earlier reaction stage. However, our measurement of Ξ^- production in $p + Nb$, presented in previous chapter, shows similar enhancement over the statistical hadronization model [31]. Fig. 10 shows the ratio of production rates of $\Xi^-(1321)$ and $\Lambda + \Sigma^0$ as a function of the total CM energy in $N + N$ collisions measured by HADES and other high-energy experiments. The reconstructed strength of the signal is compared to calculations performed for $Au + Au$ collisions with the statistical model of [41]. While high-energy data are well described, the present experimental ratio is underestimated, by the model by an order of magnitude. The similar enhancement over the statistical model observed in $p + Nb$ on seems to be in contradiction to the explanation offered for the $Ar + KCl$ case since the contribution of the multi-step processes should be negligible in $p + A$ reactions. Alternative explanation suggesting production from high mass (> 2 GeV/c^2) baryonic resonances with significant branches for the Ξ^- decay has been proposed in [32]. Furthermore, similar mechanism seems to be also instrumental for the ϕ meson production measured by HADES. However, it remains to be shown by dedicated measurements with proton-proton or pion-proton experiments that resonances with such decay indeed exist. Nevertheless, the proposed mechanism seems to be attractive since it explains not only the production of hadrons with multi-strange quark content in $p+A$ and $A+A$ reactions at low energy but also provides an interpretation for the remarkable success of the statistical hadronization description. A dedicated calculations with URQMD show that $2-3$collisions between nucleons and nucleon resonances are sufficient to produce such high mass resonances and reproduce particle yields which are consistent with predictions of statistical hadronization models [33]. It is expected that new data obtained with $Au + Au$ collisions where kaons, η, Λ and ϕ have been identified will bring another interesting insight into the production of strangeness at SIS18 energies.

In-medium effects on kaons have been studied by means of K^0_s meson transverse momentum distributions in Ar+KCl collisions at 1.76AGeV taking advantage of the good acceptance of HADES at low transverse momentum for the $K^0_s \rightarrow \pi^+\pi^-$ reconstruction [42]. We compared p_t distributions for different rapidity bins with the corresponding results by the IQMD transport approach with and without taking into account a repulsive K^0-nucleus potential. For all rapidity bins, but most evidently at mid-rapidity (shown in Fig. 11), data support calculations with the repulsive potential. Our data suggest a repulsive in-medium K^0 potential of about 40MeV which is slightly higher as compared to results obtained from experiments studying K^0_s production off nuclei [43]. Simlar studies have also been performed in $p + Nb$ collisions [44] confirming presence of a repulsive momentum-dependent kaon potential as predicted by the Chiral Perturbation Theory (ChPT). For the kaon at rest and at normal nuclear density, the ChPT potential amounts to ~ 35 MeV.

5 Conclusions

Selected results on dielectron and strangeness production in $p + Nb$ and nucleus-nucleus collisions has been reviewed.

We find that ρ meson production in our energy range is strongly affected by a strong coupling to low-mass baryonic resonances which is reflected in a significant broadening of the meson mass distribution visible in $p + A$ and $A + A$ reactions. Particularly, results from $A + A$ demonstrate a significant contribution from the dense phase of the collisions which can be successfully described by

a thermal radiation from the in-medium ρ in agreement with the higher energy data. An important verification of this scenario will be provided by $Au+Au$ data recently collected by HADES. However, also the vacuum spectral function, as concluded from $p+p$ reactions, has a non-trivial shape. It is expected that results from pion induced reactions will allow to understand details of the meson-baryon couplings and further scrutinize the underlying microscopic model of the meson-baryon interactions.

Studies of the ω production off nucleus show a strong absorption of the meson in nuclear matter in accordance with the results from photon induced reactions. The ω and ϕ signals have also been reconstructed in $Ar+KCl$ collisions at energies below the $N-N$ production threshold. A surprisingly large $R_{\phi/\omega}$ production ratio (more than one order of magnitude larger than in $N+N$ collisions) has been found, indicating no suppression for the ϕ production and consequently a significant contribution to the K^- production. The latter one is particularly surprising in view of previous interpretations assuming dominant role of strange exchange reactions. Also strong enhancements of the double strange $\Xi^-(1321)$ production above predictions of statistical hadronization models have been found as well in $p+Nb$ as in $Ar+KCl$ collisions. These intriguing results call for further experimental studies of strangeness production in his energy regime. New data obtained with $Au-Au$ system will provide additional valuable information. High purity and statistics Λ sample obtained in HADES experiment allowed also for the first studies of $\Lambda-p$ interactions in $p+A$ collisions with femtoscopy methods revealing sensitivity to disentangle repulsive and attractive contributions.

Investigations of in medium kaon potential have been performed with the measurement of K^0 production in $Ar+KCl$ and $p+Nb$ supporting a strong (U=40 MeV) repulsive potential.

The author thanks GSI Darmstadt for support for this work. The collaboration gratefully acknowledges the support by LIP Coimbra, Coimbra (Portugal) PTDC/FIS/113339/2009, UJ Kraków (Poland) NCN 2013/10/M/ST2/00042, TU München, Garching (Germany) MLL München: DFG EClust 153, VH-NG-330 BMBF 06MT9156 TP5 GSI TMKrue 1012 NPI ASCR, Rez, Rez (Czech Republic) GACR 13-06759S, NPI AS CR, Rez, USC-S. de Compostela, Santiago de Compostela (Spain) CPAN:CSD2007-00042, Goethe University, Frankfurt (Germany): HA216/EMMI HIC for FAIR (LOEWE) BMBF:06FY9100I GSI, IN2P3/CNRS (France).

References

[1] B. Friman, C. Höhne, J. Knoll, S. Leupold, J. Randrup, R. Rapp, P. Senger (editors) Lecture Notes in Physics, Vol. **814**, (2011)
[2] D. Blaschke, J.Aichelin, E. Bratkovskaya, V. Friese, M. Gazdzicki, J. Randrup, O. Rogachevsky, O. Teryaev and Viacheslav Toneev (editors) Eur. Phys. Jour. A **52**, No 8 (2016) (Topical review)
[3] L.McLerran, R. D. Pisarski Nucl.Phys. A **796** (2007) 83 Y. Hidaka, L. D. McLerran, and R. D. Pisarski, Nucl. Phys. A **808** (2008) 117
[4] K. Fukushima, Phys. Rev. D **77** (2008) 114028
[5] HADES Collaboration, EPJ Web Conf 97 (2015) 00024, EPJ Web Conf. 97 (2015) 00015
[6] G. Agakishiev et al., (HADES Collaboration), Phys. Lett.B **715**,304 (2012)
[7] R. Nasseripour et al. (CLAS Collaboration), Phys. Rev. Lett. **99** 262302 (2007)
[8] M. H. Wood et al. (CLAS Collaboration), Phys. Rev. Lett. **105** 112301 (2010)
[9] M. Naruki et al., Phys. Rev. Lett. **96** 092301 (2006)
[10] G. Agakishiev et al. (HADES Collaboration), Eur. Phys. J. A **48**, 64 (2012)
[11] J. Weil, H. van Hees and U. Mosel, arXiv:1203.3557, O. Buss et al., Phys.Rept. **512** 1 (2012)
[12] G. Ramalho, M. T Pena, J. Weil, H. van Hees, U. Mosel, Phys.Rev. **D93** 033004 (2016)

[13] G. Ramalho, M.T. Pena, Phys.Rev. D. **85**, 113014 (2012).
[14] R. Rapp and J. Wambach, Adv. Nucl. Phys. bf 25, 1 (2000).
[15] M. Nanova et al. (CBELSA-TAPS Collaboration), Phys. Rev. C **82**, 035209 (2010)
[16] J. Adamczewski-Musch et al. (HADES Collaboration) Phys.Rev. C **94** (2016) 025201
[17] J. Haidenbauer, S. Petschauer, N. Kaiser, U. G. Meissner, A. Nogga, and W. Weise, Nucl. Phys. A **915**, 24 (2013),
[18] G. Agakishiev et al. (HADES Collaboration), Phys.Rev.Lett. **114** (2015) 212301
[19] R. Averbeck et al., (TAPS Collaboration), Z. Phys. A **359**, 65 (1997)
[20] G. Agakishiev et al. (HADES Collaboration), Phys. Lett. B **690**, 118 (2010)
[21] G. Agakichiev, et al., (HADES Collaboration), Phys. Rev.C **84**, 014902 (2011)
[22] G. Agakishiev et al. (CERES Collaboration), Phys. Rev. Lett. **75** 1272 (1995)
[23] R. Arnaldi et al. (NA60 Collaboration), Phys. Rev. Lett. **96** 162302 (2006)
[24] A. Adare et al. [PHENIX Collaboration], Phys. Rev. C **93** (2016) 014904
[25] L. Adamczyk et al. (STAR Collaboration), Phys. Rev. C **92** (2015) 024912
[26] P. M. Hohler and R. Rapp, Phys. Lett. B **731** (2014) 103
[27] S. Endres, H. van Hees, J. Weil, M.Bleicher Phys.Rev. C **92**,014911(2015)
[28] R. Rapp, H. van Hees, Eur. Phys. J **52** (2016) 257
[29] T. Galatyuk, P.M. Hohler, R.Rapp, F.Seck, J.Stroth Eur. Phys. J **A52** (2016) 131
[30] G. Agakishiev et al. (HADES Collaboration), Phys. Rev. C **80**, 025209 (2009)
[31] G. Agakishiev et al. (HADES Collaboration), Eur.Phys.J.A **52** (2016) 178
[32] J.Steinheimer, M.BleicherJ.Phys. G **43** (2016) 015104
[33] J. Steinheimer, M. Lorenz, F. Becattini, R. Stock, M. Bleicher, Phys.Rev. C **93** (2016) 064908
[34] H. Schade, Gy. Wolf, B. Kämpfer, Phys. Rev. C **81**, 034902 (2010)
[35] S. Wheaton, J. Cleymans, and M. Hauer, Comput. Phys. Commun. **180**, 84 (2009)
[36] G. Agakishiev et al. (HADES Collaboration), Eur. Phys. J. A **47**, 21 (2011)
[37] G. Agakishiev et al. (HADES Collaboration), Phys. Rev. Lett **103**, 132301 (2009)
[38] K. Fukushima, Eur. Phys. J. A **52** (2016) 222
[39] C. M. Ko et. al, Phys. Rev. C **85**, 064902 (2012).
[40] E. E. Kolomeitsev, B. Tomasik, and D. N. Voskresensky, Phys. Rev. C **86**,(2012)054909
[41] A. Andronic, P. Braun-Munzinger, and K. Redlich, Nucl. Phys. A **765**, 211 (2006)
[42] G. Agakishiev et al. (HADES Collaboration), Phys. Rev. C **82**, 044907 (2010)
[43] M.L. Benabderrahmane et al. (FOPI), Phys. Rev. Lett. **102**, 182501 (2009)
[44] G. Agakishiev et al. (HADES Collaboration), Phys.Rev. C **90** (2014) 054906